JAMES | Journal of Advances in Modeling Earth Systems

RESEARCH ARTICLE
10.1029/2019MS001685

Surface Flux Equilibrium Theory Explains an Empirical Estimate of Water-Limited Daily Evapotranspiration

Kaighin A. McColl[1,2], **Guido D. Salvucci**[3], **and Pierre Gentine**[4]

[1]Department of Earth and Planetary Sciences, Harvard University, Cambridge, MA, USA, [2]School of Engineering and Applied Sciences, Harvard University, Cambridge, MA, USA, [3]Department of Earth and Environment, Boston University, Boston, MA, USA, [4]Department of Earth and Environmental Engineering, Columbia University, New York, NY, USA

Key Points:
- Empirical work suggests that ET can be estimated from atmospheric observations alone, even under water-limited conditions
- We develop an idealized equilibrium ET-ABL model that couples the surface and atmospheric states
- The model reproduces and explains the observed phenomenon

Correspondence to:
K. A. McColl,
kmccoll@seas.harvard.edu

Citation:
McColl, K. A., Salvucci, G. D., & Gentine, P. (2019). Surface flux equilibrium theory explains an empirical estimate of water-limited daily evapotranspiration. *Journal of Advances in Modeling Earth Systems*, *11*. https://doi.org/10.1029/2019MS001685

Received 12 MAR 2019
Accepted 6 JUN 2019
Accepted article online 11 JUN 2019

Abstract Evapotranspiration (ET) plays a central role in the water, energy, and carbon cycles but is difficult to model and estimate due to its dependence on the heterogeneous land surface. Recent studies suggest that standard weather station atmospheric observations alone may be sufficient to estimate ET. This is surprising since ET over land is often strongly constrained by the land surface, for instance, by water limitation. While these studies have been empirically successful, a physical explanation for why this is possible has been lacking. Here, we provide a physical explanation for why one of these approaches—the ET from Relative Humidity at Equilibrium (ETRHEQ) method—works, using a simple model of a steady-state idealized atmospheric boundary layer. We show that, across a wide range of plausible parameter values, this model reproduces ETRHEQ, suggesting that it contains the essential physics that lead to ETRHEQ. We derive a closed-form expression for ETRHEQ at steady state and use it to show that ETRHEQ can be explained in terms of the near-surface relative humidity (RH) budget of the idealized model: in particular, it is equivalent to assuming a balance between surface moistening and heating terms in the RH budget. Negative feedbacks between surface fluxes (constrained by the surface energy budget) and atmospheric temperature and humidity mean that these terms typically balance, explaining the empirical success of ETRHEQ over a wide range of conditions. We define this state—in which the moistening and heating terms balance in the RH budget—as "surface flux equilibrium."

1. Introduction

Evapotranspiration (ET, the sum of evaporation E and transpiration T) is a major component of the water cycle, the energy cycle (due to evaporative cooling), and the carbon cycle (due to coordination between transpiration and photosynthesis in plants (Green et al., 2019; Humphrey et al., 2018)). Estimating ET over inland continental regions is of particular interest because this is where climate models are particularly prone to failure (e.g., Ma et al., 2018). An inherent challenge in modeling ET is that the land surface is extremely heterogeneous. Since ET is a function of both the land surface and the atmosphere, it is difficult to parameterize (Monteith, 1965). Approaches that do not require explicit parameterization of land surface conditions are, therefore, desirable.

Under special conditions, ET reaches an interesting "equilibrium" value that does not explicitly depend on surface conditions. While there are various definitions of equilibrium ET, arguably the most fundamental (Raupach, 2001) is the evaporative state achieved by a closed system—forced with constant incoming radiation that is partitioned at the lower boundary between latent and sensible heat fluxes—that is allowed to evolve to a quasi-equilibrium state in which the vapor pressure deficit (VPD) is constant (McNaughton, 1976a, 1976b; Slatyer & McIlroy, 1961). The eventual quasi-equilibrium ET in this system, regardless of surface water limitation or initial conditions, is

$$\lambda E = \frac{\epsilon}{\epsilon + 1}(R_n - G) \tag{1}$$

where $\epsilon = \Delta\lambda/c_p$, $\Delta = \left.\frac{\mathrm{d}q^*}{\mathrm{d}T}\right|_{T=\theta_M}$, θ_M is screen-level potential temperature, λ is the latent heat of vaporization of water, c_p is the specific heat capacity of air, R_n is net radiation, and G is ground heat flux. This result is significant since, given enough time (with more time required for more surface-limited conditions), the system evolves to a state in which ET is solely a function of the atmospheric state ($\epsilon(\theta_M)$) and available energy

($R_n - G$). Any surface limitation (e.g., water limitation) eventually becomes encoded in the atmospheric state and does not enter equation (1) explicitly.

In the real world, however, the system is not closed. If the control volume is a convective boundary layer (CBL), then on time scales of hours, relatively dry and warm air is entrained at the top of the CBL, increasing its VPD and ET relative to the equilibrium value (De Bruin, 1983; McNaughton & Spriggs, 1986). This effect is typically modeled empirically by multiplying the equilibrium value by the Priestley-Taylor parameter, α (Priestley & Taylor, 1972). This value is often taken to be 1.26, based on the original field study, which agrees reasonably with plausible model predictions (Culf, 1994; De Bruin, 1983; Raupach, 2000), although values of α have been observed that depart from this value considerably (Shuttleworth & Calder, 1979). Despite the success of these methods, they are fundamentally restricted to well-watered surfaces: the time to equilibrium increases with increasing surface limitation, meaning equilibrium is rarely achieved in the temporally varying real world, unless surface limitation is small (Raupach, 2000, 2001). Therefore, these approaches are incapable of modeling ET over most land surfaces. While efforts to model α as a function of surface conditions (e.g., De Bruin (1983)) have been useful for developing physical understanding, they still require knowledge of surface conditions if they are to be applied to estimate ET over water-limited land surfaces.

Can equilibrium approaches be devised that allow ET to be estimated over water-limited surfaces *without explicitly parameterizing surface limitation*? While the land and atmosphere are tightly coupled, it seems reasonable to hypothesize that the near-surface atmosphere responds more rapidly to perturbations compared to the land surface; this implies that, at some time scale, the near-surface atmosphere will reflect the state of the land surface, regardless of surface limitation (Novick et al., 2016; Zhou et al., 2019), and therefore, atmospheric observations alone should be sufficient to estimate ET. Recent approaches broadly based on this idea—that atmospheric observations alone contain sufficient information to estimate ET—have proven empirically successful even under conditions where surface conditions limit ET (Gentine et al., 2013, 2016; Salvucci & Gentine, 2013). This is a major advantage since weather station data are relatively plentiful compared to land surface observations of parameters controlling surface limitation (e.g., soil moisture). In particular, the ETRHEQ (ET from Relative Humidity at Equilibrium) method parameterizes the surface conductance based on a hypothesized relation between surface conductance and RH, namely, that the true surface conductance (assumed constant over the course of a day) minimizes the vertical variance of the RH profile averaged over the day (Rigden & Salvucci, 2015, 2017; Salvucci & Gentine, 2013).

However, there is currently no physical explanation for why such empirical weather station based estimates work. Previous studies (Salvucci & Gentine, 2013) have speculated that this is a result of an "equilibrium" state. However, no mechanistic model has so far been proposed that explains this phenomenon. Here, we propose an idealized model of the atmospheric boundary layer (ABL) that reproduces ETRHEQ. The model's simplicity allows us to identify the most fundamental physical mechanisms that govern this equilibrium, in particular, that ETRHEQ is equivalent to assuming a balance between the surface heating and moistening terms in the steady-state relative humidity budget, a state we call "surface flux equilibrium" (SFE).

This manuscript is structured as follows. We first summarize the ETRHEQ method. Next, we introduce a simple steady-state box model of the ABL and demonstrate that it reproduces ETRHEQ. An explanation is then provided in terms of the steady-state ABL relative humidity budget. Finally, limitations and implications are discussed.

2. The ETRHEQ Hypothesis

ET is partly constrained by hydrologic and biophysical mechanisms at the land surface. A "big leaf" formulation for evaporation reads as (Monteith, 1981)

$$E = \rho \frac{g_s g_a}{g_s + g_a} \left(q^*(T_S) - q_M \right) \tag{2}$$

where g_s is the surface conductance, g_a is the aerodynamic conductance, $q^*(T_S)$ is the saturation specific humidity evaluated at the surface temperature, and q_M is the screen-level (often taken as 2 m above the surface) specific humidity. The surface conductance g_s is particularly difficult to parameterize, since it is a function of the heterogeneous land surface, and reflects limitations due to water availability, plant

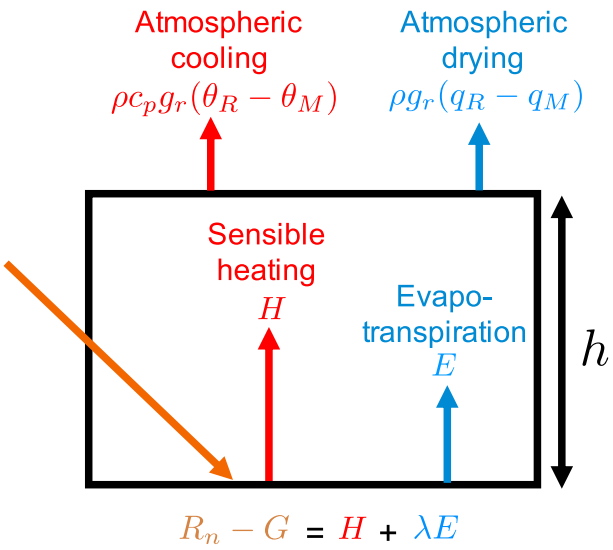

Figure 1. Schematic of the idealized box model of the atmospheric boundary layer. The box has depth h. R_n is net radiation (the difference between incoming and outgoing radiation at the surface). G is the ground heat flux. H and λE are sensible and latent heat fluxes, respectively. The box has potential temperature θ_M and specific humidity q_M. g_r is the atmospheric cooling and drying conductance. q_R and θ_R are the relaxation specific humidity and temperature, respectively. ρ is the density of air, and c_p is the specific heat capacity of air.

physiology, and land use. However, for simplicity, we use the terms "surface limited" and "water limited" interchangeably in this study.

The weather station ET estimate, ETRHEQ, hypothesizes that the true value of g_s minimizes the vertical variance of the RH profile, averaged over the course of the day (Rigden & Salvucci, 2015, 2017; Salvucci & Gentine, 2013). This implies that g_s can be estimated using weather station data, with almost no information on the land surface required (an estimate of vegetation height is the only necessary land surface input). More specifically, ETRHEQ hypothesizes that the true value of g_s (defined here as $\bar{g}_s$) satisfies the condition (Rigden & Salvucci, 2017)

$$\frac{\partial}{\partial g_s}\left[\frac{1}{T}\int_0^T (RH_S(t,g_s) - RH(t))^2 \mathrm{d}t\right]\Bigg|_{g_s=\bar{g}_s} = 0 \tag{3}$$

where $RH_S = q_S/q^*(T_S)$. For a steady-state case, the ETRHEQ condition simplifies to

$$\frac{\partial[(RH_S(g_s) - RH)^2]}{\partial g_s}\Bigg|_{g_s=\bar{g}_s} = 0 \tag{4}$$

In Appendix A, we provide a derivation showing that, for the steady-state case, this expression simplifies substantially to a closed-form expression for the evaporative fraction (EF)

$$EF \equiv \frac{\lambda E}{R_n - G} = \frac{RH\epsilon}{RH\epsilon + 1} \tag{5}$$

where $RH = q_M/q^*(T_M)$ is the atmospheric relative humidity.

However, while ETRHEQ has been empirically successful (Rigden & Salvucci, 2015; Salvucci & Gentine, 2013), a physical explanation is lacking. The ETRHEQ hypothesis is a useful approximation but is unlikely to hold exactly, implying that it is unlikely that it can be derived exactly from the governing equations. Instead, we propose a simple model of the ABL that reproduces the ETRHEQ hypothesis to the same level of accuracy as observed empirically. We choose the model to be as simple as possible, while still retaining clear conceptual links to the real ABL. As we will show, the model's simplicity facilitates physical insight and the development of intuition that would not be possible with more complex models.

3. A Box Model of the Steady ABL

The concept of equilibrium ET is fundamentally based on a closed box model (Raupach, 2001). We parsimoniously build on this model in this study, resulting in a model that can be interpreted as a conceptual model of the diel-average ABL (i.e., the ABL averaged over a full day-night cycle). The model consists of a box, forced with constant incoming shortwave and longwave radiation, which can be interpreted as daily averages (Figure 1). In analogy with the ABL, the box is assumed to be well mixed, implying that vertical gradients of potential temperature and specific humidity are zero.

The energy and moisture budgets for the box model are as follows:

$$\frac{\mathrm{d}\theta_M}{\mathrm{d}t} = \frac{H}{\rho c_p h} + \frac{g_r}{h}(\theta_R - \theta_M) \tag{6}$$

$$\frac{\mathrm{d}q_M}{\mathrm{d}t} = \frac{\lambda E}{\rho \lambda h} + \frac{g_r}{h}(q_R - q_M) \tag{7}$$

where θ_M is the box potential temperature, t is time, h is the height of the box, H and λE are sensible and latent heat fluxes, respectively, g_r is the conductance of the generic atmospheric cooling and drying terms, and θ_R and q_R are reference temperature and specific humidity, respectively (explained below). While latent

Table 1
Parameter Values and Ranges Used in the Sensitivity Analysis

Variable	Baseline value	Sensitivity test range	Unit
Aerodynamic conductance g_a	1/50	1/200–1/10	m/s
Surface conductance g_s	1/900	1/900–1/60	m/s
Ground heat flux reference temperature T_g	8	0–20	°C
Ground heat flux conductivity k_g	0.3	0–2	$J{\cdot}m^{-1}{\cdot}s^{-1}{\cdot}K^{-1}$
Downwelling shortwave radiation F_{sd}	700	300–1300	W/m^2
Downwelling longwave radiation F_{ld}	300	100–700	W/m^2
Surface albedo a_s	0.5	0–1	—
Boundary layer height h	1,000	50–1500	m
Atmospheric cooling relaxation temperature θ_R	10	0–15	°C
Atmospheric drying relaxation specific humidity q_R	10^{-3}	$0–3 \times 10^{-3}$	kg/kg
Relaxation conductance g_r	h/(10 days)	Fixed	m/day

heating is a more efficient method of heat dissipation under typical daytime warm and wet conditions (Bateni & Entekhabi, 2012), it is often constrained at the land surface by water limitation and other factors. The air temperature and specific humidity in the box increase in response to H and E, respectively. A generic cooling flux balances the surface heating, and a drying flux balances the surface moistening from E. Both terms are represented as linear relaxation terms, in which the box temperature and specific humidity are both relaxed back to a reference temperature and reference specific humidity, respectively, over the time scale h/g_r. Linear relaxations are commonly used forms (e.g., see Byrne & O'Gorman, 2016, for atmospheric drying and Pauluis & Held, 2002, for atmospheric cooling). These fluxes ensure that the model reaches equilibrium. Plausible examples of cooling fluxes in the ABL include radiative cooling, or cooling from convective downdrafts. Examples of drying fluxes include dry air entrainment or convective ventilation through cloud base mass flux.

The incoming energy is partitioned at the surface between sensible heat H and latent heat λE according to

$$R_n - G = H + \lambda E \tag{8}$$

where the net radiation $R_n = (1 - a_s)F_{sd} + F_{ld} - \epsilon\sigma T_S^4$, where surface emissivity $\epsilon = 0.98$, T_S is surface temperature, and other terms are defined in Table 1. The ground heat flux is modeled as $G = k_g(T_S - T_g)/d_g$, where the depth to a deep soil layer with constant temperature T_g is $d_g = 1$ m (Raupach, 2001). Other parameters are defined in Table 1. The turbulent fluxes are given by

$$H = \rho c_p g_a (T_S - \theta_M) \tag{9}$$

$$\lambda E = \rho\lambda \frac{g_a g_s}{g_a + g_s}(q^*(T_S) - q_M) = \rho\lambda g_s (q^*(T_S) - q_S) \tag{10}$$

where g_a is atmospheric conductance and q_S is specific humidity at the surface. For simplicity, we ignore impacts of thermal stratification on g_a. The equations are nonlinear since the equation for λE includes the saturation specific humidity $q^*(T_s)$, a nonlinear function of temperature given by the Clausius-Clapeyron relation. If T_s is held constant, then $q^*(T_s)$ is also constant and the equations can be solved analytically, but this is not the case for our simulations, where T_s is allowed to evolve freely in time.

The model is run to steady state (Betts, 2000). ETRHEQ simplifies substantially at steady state (equation (5)), so we focus on the steady state case in this study. Consistent with previous box models used to study equilibrium ET, its height is fixed to be h (Betts, 1994; Culf, 1994; Raupach, 2000, 2001). While diurnal variability is significant in the ABL over land, our box model can be interpreted as approximately averaging over this variability on multiday time scales, similar to previous equilibrium models, which have been used to yield insights into the coupling with the land surface on longer time scales (Betts, 2000; Betts & Chiu, 2010; Cronin, 2013; Raupach, 2001). The results of our analysis are robust to large changes in h (and other parameters), as described below. We further discuss this simplification in section 6.

The model presented here is most similar to that given in Raupach (2000). One key difference is that we exclude an entrainment warming term. This term is typically small: most of the extra heat energy entrained from the free troposphere is used to grow the boundary layer rather than warm it (Driedonks, 1982), and since we prescribe a fixed height for our steady model, it can be safely ignored. The entrainment warming term is effectively replaced by an atmospheric cooling term, which becomes significant at multiday time scales (we describe these differences further in section 6). For numerically solving the equations, we include in equations (9) and (10) additional terms relating to condensation (parameterized as in Vallis et al., 2019). These are required to numerically integrate the equations across a wide range of parameters but are not physically significant in the cases we consider, so are not shown in equations (9) and (10).

The governing equations for the atmosphere can be nondimensionalized to give

$$\frac{\mathrm{d}\hat{\theta}_M}{\mathrm{d}\hat{t}} = \hat{H} + \frac{g_r}{g_a}(\hat{\theta}_R - \hat{\theta}_M) \tag{11}$$

$$\frac{\mathrm{d}\hat{q}_M}{\mathrm{d}\hat{t}} = \lambda\hat{\mathrm{E}} + \frac{g_r}{g_a}(\hat{q}_R - \hat{q}_M) \tag{12}$$

where $\hat{q} = q\rho\lambda g_a/(R_n - G)$, $\hat{t} = tg_a/h$, and $\hat{T} = T\rho c_p g_a/(R_n - G)$.

The system evolves to an equilibrium state for a given forcing and parameters when $g_r \neq 0$. The equilibrium ABL state (θ_M, q_M) can be thought of as a mixture of the equilibrium surface state $(T_s, q^*(T_s))$ and reference state (θ_R, q_R). The relative weighting of this mixture is determined by g_r/g_a: small g_r/g_a means the equilibrium ABL state is closer to the equilibrium surface state, whereas high g_r/g_a means the equilibrium ABL state is closer to the reference state. Alternatively, g_r/g_a can be interpreted as the inverse sensitivity of the equilibrium ABL state to changes in surface fluxes:

$$\frac{\partial\hat{q}_M}{\partial\lambda\hat{\mathrm{E}}} = \frac{\partial\hat{\theta}_M}{\partial H} = \frac{1}{g_r/g_a} \tag{13}$$

Therefore, for small g_r/g_a, the idealized ABL is more like a greenhouse: the ABL state is highly sensitive to changes in surface fluxes, meaning surface fluxes largely determine the ABL state. In contrast, for large g_r/g_a, the ABL state is insensitive to changes in surface fluxes, meaning the ABL state is largely imposed by the external atmosphere. This is conceptually similar to the decoupling parameter framework of Jarvis and McNaughton (1986). While we would expect g_r to be anticorrelated with θ_R and q_R, equation (13) shows that g_r determines the sensitivity of the atmospheric state to surface fluxes, independent of θ_R and q_R.

4. The Box Model Reproduces ETRHEQ

A sensitivity analysis is performed by varying model parameters one at a time (Table 1). Values of g_a and g_s are chosen to be similar to those used in the sensitivity tests of Betts (2000). The relaxation conductance g_r is more difficult to constrain. In this study, it is chosen to be a fixed function of h: $g_r = h/(10\ \text{days})$. This choice effectively imposes a residence time of 10 days on water vapor in the ABL. This drying time scale has been used commonly in the literature over oceans (Deremble et al., 2012; Emanuel & Zivkovic-Rothman, 1999; Seager et al., 1995) and also as a synoptic forcing time scale over land (D'Andrea et al., 2006). It is possible that the true residence time might be lower than this estimate. However, the main results of this study are robust to substantial variations in this parameter; for example, the results are qualitatively similar if the imposed residence time is halved to 5 days. The chosen parameters result in a realistic amount of cooling if the atmospheric cooling term is interpreted as a radiative cooling rate: for the baseline case, the effective cooling is −2.3 K/day (Betts, 2000).

For a given set of initial conditions and parameters, the box model converges to a steady state (Figure 2), yielding a time series of synthetic truth λE, specific humidity, and air temperature. At steady state, the model air temperature and specific humidity can be used as inputs to ETRHEQ (equation (5)) to estimate λE. If this estimate is a reasonable approximation of the synthetic truth λE across a wide range of parameter choices, it suggests (but does not guarantee) that the model contains the fundamental physics that explain ETRHEQ.

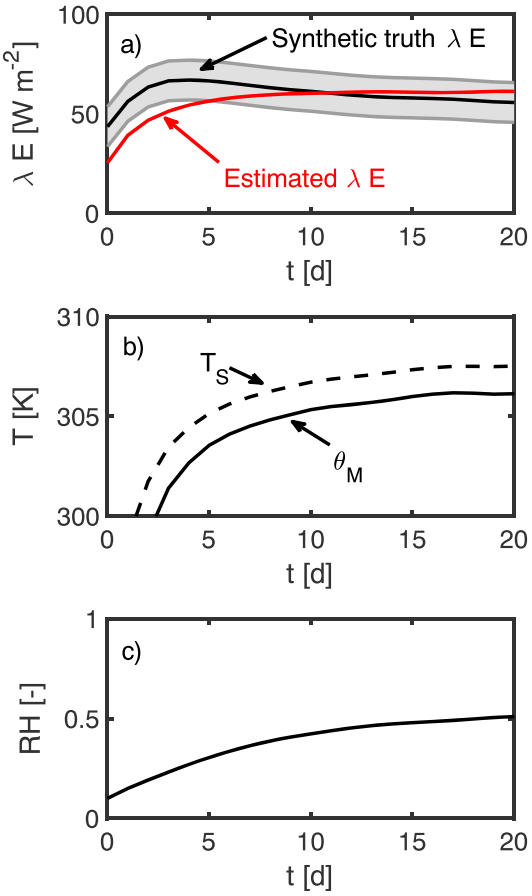

Figure 2. Example behavior of the box model in the baseline case used in the sensitivity test. (a) Traces of synthetic truth λE (solid black line) and ETRHEQ estimated λE (equation (5), red solid line). The shaded region is ± 10 W/m^2, representing a (conservatively low) uncertainty estimate on eddy covariance measurements of λE (Aubinet et al., 2012). (b) Traces of surface temperature T_S (black dashed line) and air potential temperature θ_M (black solid line). (c) Trace of screen-level relative humidity RH.

There is no reason to believe that the hypothesis behind ETRHEQ is an exact result, and we do not expect there to be zero error.

The steady-state λE estimated by ETRHEQ (equation (5)) reasonably matches the synthetic truth λE, across a broad range of parameter choices (Figure 3a). More specifically, for the parameter ranges given in Table 1, the ETRHEQ estimate of E has a root-mean-square error (RMSE) of 9.6 cm/year. This compares favorably with the comparison with field data given in Figure 3 of Rigden and Salvucci (2015), where the ETRHEQ RMSE when compared with field observations is 11.6 cm/year. A higher RMSE is expected when compared with field observations, since they are subject to measurement error.

ETRHEQ has the largest absolute errors when available energy is highest (Figure 4). This corresponds to cases where downwelling longwave radiation F_{ld} and/or downwelling shortwave radiation F_{sd} are high, when surface albedo a_s is low, and/or when ground heat flux conductivity k_g is low (implying a small ground heat flux). In these cases, there is more energy available to be partitioned between the turbulent fluxes (sensible and latent heat). These typically correspond to cases where E is relatively high in Figure 3, meaning relative errors are still quite low. In addition, the errors are somewhat sensitive to choice of reference temperature used in the atmospheric cooling term θ_R (Figure 4). However, constraining θ_R to a range in which the atmospheric cooling term produces values that could plausibly be interpreted as radiative cooling terms (following Betts, 2000, -1 to -3 K/day) results in low errors.

ETRHEQ performs substantially better than the classical equilibrium model given in equation (1) (Figure 3b). The classical equilibrium model is most appropriate for well-watered surfaces, since the time

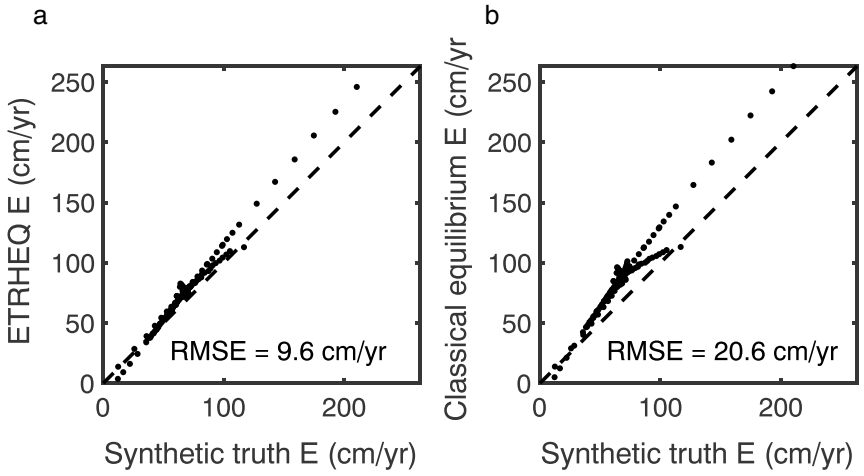

Figure 3. Scatter plot comparisons—for each set of parameters used in the sensitivity test—between synthetic truth E and (a) ETRHEQ-estimated E (equation (5)) and (b) classical equilibrium E (equation (1)). RMSE is root-mean-square error in estimated E evaluated over all parameter sets used in the sensitivity analysis. Dashed line is the 1:1 line. ETRHEQ = ET from Relative Humidity at Equilibrium.

to equilibrium is much longer than real-world weather variability time scales when the surface is water limited, meaning an equilibrium state is typically not realized (McNaughton, 1976a, 1976b; Raupach, 2001; Slatyer & McIlroy, 1961). We refer to equation (1) as "classical equilibrium" ET in the remainder of the paper. When g_s is high and surface conditions are not limiting, the ETRHEQ (equation (5)) and classical equilibrium (equation (1)) solutions both have similarly low errors (Figure 4). However, as $g_s \to 0$, errors in the classical equilibrium solution grow substantially compared to errors in the ETRHEQ solution. The box model on which the classical equilibrium estimate of ET is based (Raupach, 2001) is a special case of our model, where $g_r = 0$. In this case, ETRHEQ and the classical estimate have similarly low errors (Figure 4). However, in this case, the box continues to get wetter and warmer with time, rather than reaching a steady state. It approaches saturation ($RH \to 1$), in contrast to the observed ABL, where $RH < 1$ in most cases. One of the reasons for this difference is vertical mixing with the upper troposphere, which dries the box, and general atmospheric cooling, which can include radiative cooling and cooling from convective downdrafts (Emanuel, 1995; Raymond, 1995). These processes are represented by $g_r > 0$. As they become more vigorous (i.e., g_r grows larger), the ETRHEQ solution continues to maintain low errors, whereas errors in the classical equilibrium ET estimate grow (as we will see in the next section, g_r must still remain small compared to g_a for errors in ETRHEQ to remain small, but this is usually satisfied in most cases in the ABL). Overall, ETRHEQ (equation (5)) accurately estimates λE within the box model and much more accurately than the classical equilibrium model (equation (1)). This suggests that the box model contains the most important physics that explain ETRHEQ.

5. Surface Flux Equilibrium

In this section, we present an explanation for ETRHEQ based on terms in the RH budget. Previous studies of classical equilibrium ET (equation (1)) have focused on the VPD budget (e.g., McNaughton & Spriggs, 1986; Raupach, 2000, 2001). RH is related to VPD but contains different information and is more relevant to ETRHEQ, which is based on a hypothesis about the gradient of RH. We discuss previous studies in more detail in section 6.

The nondimensionalized relative humidity budget is (see Appendix B for a derivation)

$$\hat{q}^*(\theta_M)\frac{\mathrm{d}\hat{RH}}{\mathrm{d}\hat{t}} = \overbrace{\lambda\hat{\mathrm{E}}}^{\text{I: surface moistening}} - \overbrace{\hat{RH}\hat{\Delta}\hat{H}}^{\text{II: surface heating}} + \frac{g_r}{g_a}\left(\overbrace{(\hat{q}_R - \hat{q}_M)}^{\text{III: atmospheric drying}} - \overbrace{\hat{RH}\hat{\Delta}(\hat{\theta}_R - \hat{\theta}_M)}^{\text{IV: atmospheric cooling}}\right) \quad (14)$$

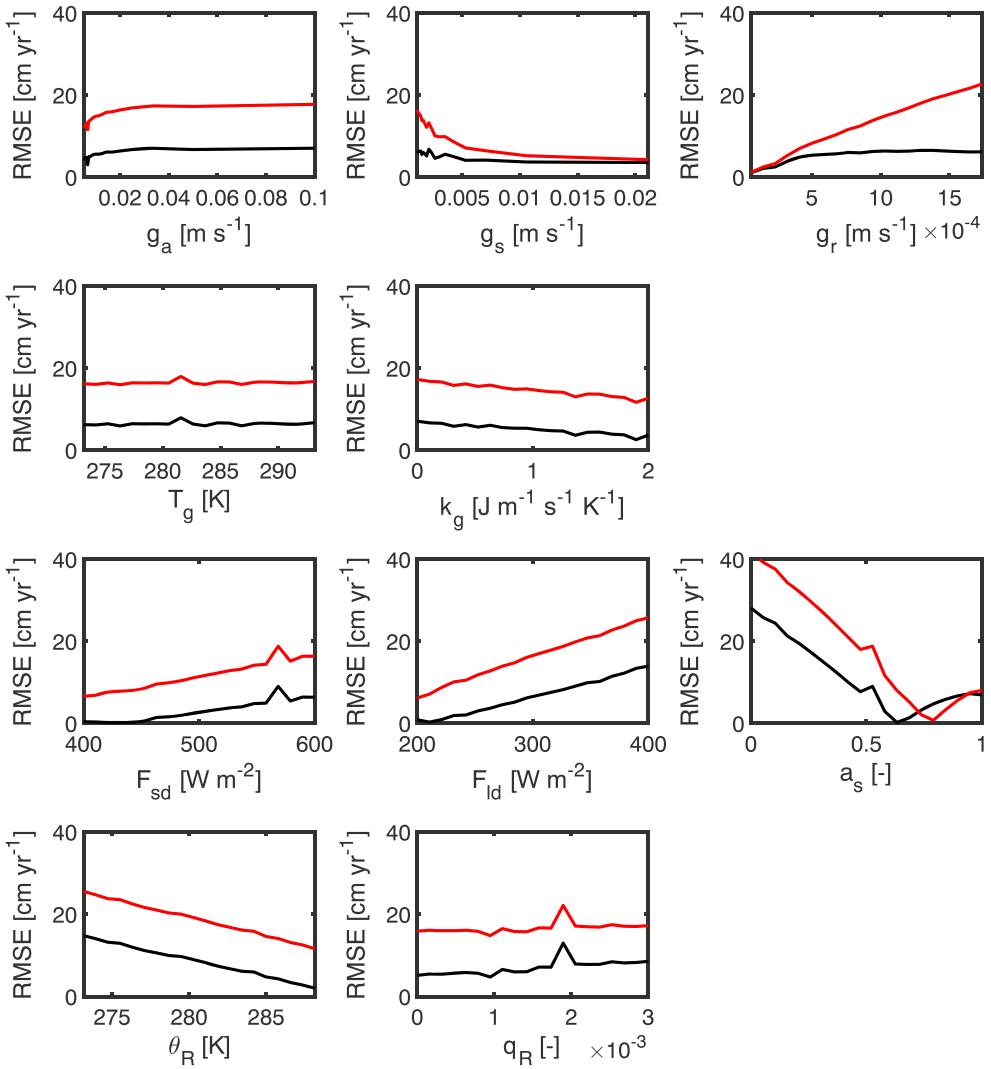

Figure 4. Dependence of errors for ETRHEQ (solid black line) and classical equilibrium E (red solid line) on parameters defined in Table 1. Errors are root-mean-square differences between synthetic truth E and ETRHEQ E (equation (5)). Parameters are set to their baseline values defined in Table 1 and varied one at a time in each subplot.

Recall that, for the case where g_r/g_a is small, the equilibrium ABL state is largely determined by surface fluxes. If evaporation is large (implying that sensible heating is relatively small), then its equilibrium specific humidity will be relatively high and its equilibrium temperature will be relatively low. Its equilibrium RH will, therefore, be relatively high. Since the surface heating term in the RH budget includes the product of RH and the sensible heat flux, the relatively small sensible heat flux will be amplified by the relatively high RH, resulting in the approximate balance of the surface moistening and surface heating terms in the RH budget (terms I and II in equation (14), respectively)

$$\lambda\hat{\mathrm{E}} \approx \hat{R\mathrm{H}}\hat{\Delta}\hat{H} \tag{15}$$

Combining the definition of EF with equation (15) yields

$$EF \equiv \frac{1}{1+\frac{\hat{H}}{\lambda\hat{\mathrm{E}}}} = \frac{\hat{R\mathrm{H}}\hat{\Delta}}{\hat{R\mathrm{H}}\hat{\Delta}+1} = \frac{RH\epsilon}{RH\epsilon+1} \tag{16}$$

This expression is exactly equivalent to ETRHEQ at steady state (equation (5)). Therefore, the ETRHEQ relation can be interpreted as a balance between surface moistening and heating terms in the relative humidity budget. We call this approximation (equation (15)) "surface flux equilibrium" (SFE).

For the special case where $g_r = 0$, the box no longer includes cooling or drying terms. It does not reach a steady state, continuing to get hotter and moister with time. In this case, the box eventually reaches saturation ($RH \to 1$; note that this is consistent with Raupach, 2001, equation 37, since $p \to 0$ as $t \to \infty$, using his notation). Therefore, ETRHEQ (equation (5)) becomes equivalent to the classical equilibrium solution (equation (1)). The classical equilibrium solution was derived in Raupach (2001) for a closed box model, using a VPD budget. Our work can be thought of as generalizing that of Raupach (2001) (and similar studies) to surface-limited conditions. We make further comparisons with previous studies in section 6.

For the case where g_r/g_a is large, the equilibrium ABL state is relatively insensitive to surface fluxes. In this case, SFE does not hold, and ETRHEQ no longer provides a good estimate of *EF*. This is confirmed by our model (not shown). Since the atmospheric drying and cooling terms are not connected by an equivalent to the surface energy balance, there is no equivalent state to SFE, in which the atmospheric drying and cooling terms (terms III and IV, respectively, in equation (14)) balance. However, at multiday time scales, g_r/g_a is small, and so this case occurs infrequently.

In summary, the surface moistening and heating terms in the RH budget approximately balance over a wide range of conditions when g_r/g_a is small, which explains ETRHEQ. Our analysis of the RH budget is consistent with a previous LES study (van Stratum et al., 2014), where it was found that the surface moistening and warming terms approximately balanced in the budget of relative humidity, albeit evaluated in this case at the top of the boundary layer rather than at the surface. Previous studies over ocean have often used fixed sea surface temperatures as the lower boundary condition (e.g., Rieck et al., 2012; Blossey et al., 2013). While these studies have provided useful insights, they do not necessarily close the surface energy budget, perhaps explaining why this result has not been identified previously.

6. Discussion

In the absence of other constraints (such as water limitation or the closing of stomata), ET is known to increase with increasing VPD and therefore decrease with increasing RH. However, the simplified expression for EF (equation (16)) implies EF increases with increasing RH. The explanation for this apparent contradiction lies in the different time scales in each case. ET increases with decreasing RH instantaneously, meaning ET is anticorrelated with RH at short time scales. However, over longer time scales, large RH is the result of large ET, meaning ET and RH are positively correlated (Betts, 2000).

A theory of "boundary layer equilibrium" (BLE) was proposed by Raymond (1995) and Emanuel (1995). In this theory, an equilibrium boundary layer equivalent potential temperature is maintained by a negative feedback between surface fluxes and convection: surface fluxes increase boundary layer equivalent potential temperature, triggering convection and downdrafts, which decrease boundary layer equivalent potential temperature. SFE is distinct from BLE. For example, BLE can still hold in models with fixed surface temperatures (where the surface energy balance is not necessarily enforced). In contrast, SFE requires enforcement of the surface energy balance at the lower boundary.

6.1. Comparison With Previous Studies of Equilibrium ET

SFE departs from previous studies of equilibrium ET in two major respects. First, previous studies mainly focused on shorter time scales relevant to the morning growth of a CBL (De Bruin, 1983; McNaughton & Spriggs, 1986; Raupach, 2000; van Heerwaarden et al., 2009), in which g_r/g_a is not small, a requirement of SFE. The growth of the CBL occurs on time scales of hours. Surface heating grows the boundary layer, leading to entrainment of air from the free troposphere. In this case, $g_r = \mathrm{d}h/\mathrm{d}t$, and θ_R and q_R are potential temperature and specific humidity of the free troposphere, respectively, and can be specified by a reference profile that varies with height. To represent the rapid entrainment of relatively warm and dry air, in this case, $\theta_R > \theta_M$, $q_R < q_M$ and $g_r/g_a \sim 1$. Since g_r and g_a are comparable in magnitude, the equilibrium state of the CBL is not dominated by either the surface or reference (in this case, the free troposphere) states. It has been shown that the equilibrium λE in this case is greater than the equilibrium value (equation (1)), due to mixing of dry, warm air from the free troposphere, which stimulates further ET. This work has led to considerable insight about ET in the CBL but is not relevant to SFE, which applies when $g_r/g_a \ll 1$, making it more appropriate for longer time scales. On time scales of days to weeks, slower mechanisms other than entrainment become more significant in setting the diel-average state of the ABL. For example, radiative cooling is slow and plays a relatively minor role in the growth of the CBL but becomes significant on longer time scales.

Second, previous studies have focused on the VPD budget rather than the RH budget. For the box model we consider, the equivalent VPD budget is

$$-\frac{\mathrm{d}\hat{D}}{\mathrm{d}\hat{t}} = \overbrace{\lambda\hat{\mathrm{E}}}^{\text{I: surface moistening}} - \overbrace{\hat{\Delta}\hat{H}}^{\text{II: surface heating}} + \frac{g_r}{g_a}\left(\overbrace{(\hat{q}_R - \hat{q}_M)}^{\text{III: atmospheric drying}} - \overbrace{\hat{\Delta}(\hat{\theta}_R - \hat{\theta}_M)}^{\text{IV: atmospheric cooling}}\right) \tag{17}$$

where D is VPD. One advantage of the VPD budget is that it can be written in terms of $\hat{D}$ alone, resulting in a closed-form solution for D and λE Raupach (2000). However, the resulting closed-form solution for λE is a function of g_s, requiring information on surface properties, which we would like to avoid. A major disadvantage of the VPD budget is that the surface heating and moistening terms do not balance, in general, as they approximately do in the RH budget, because the surface heating term does not include modulation by RH. Therefore, even if g_r/g_a is small, SFE cannot be obtained from the VPD budget, the focus of previous studies.

6.2. Limitations

Important caveats apply to our theory. Many land surfaces are not in a state of SFE, for example, regions with substantial moisture or heat convergence. It has been noted in previous studies that ETRHEQ performs poorly empirically in regions near coasts where moisture convergence is expected to be significant (Rigden & Salvucci, 2015; Salvucci & Gentine, 2013), consistent with our theory. It is also possible that convective precipitation might increase g_r/g_a to an extent that SFE does not hold. Nevertheless, based on the fact that ETRHEQ performs well empirically across a wide range of locations and conditions, it suggests that SFE may be a reasonable approximation of reality at the daily or multiday time scale for many inland continental areas, even in the presence of some convective precipitation. It is precisely these regions that are subject to large errors in near-surface air temperatures in models, with underestimated EF a main driver of this error (Ma et al., 2018). The SFE framework may potentially be useful in correcting these errors in models.

We use a conceptual model of the diel-average ABL and do not attempt to model the diurnal cycle. An alternative approach would be to integrate the prognostic equations for the ABL in time and then average the outputs over a diel cycle rather than conceptually modeling the diel-average state of the ABL directly. We choose the latter approach for several reasons. First, the aim of this study is to explain the empirical success of ETRHEQ using a maximum simplicity model. Integrating the equations over a diel cycle requires knowledge of the physics governing the nocturnal stable ABL. While significant strides have been made on this problem, the physics of the nocturnal ABL are still relatively poorly understood. In our view, the benefits of more realistic physics obtained from integrating the prognostic equations over a diel cycle do not outweigh the additional cost of model complexity, particularly given the uncertainty in nocturnal ABL processes. Second, in the sensitivity analysis, we demonstrate that our box model reproduces ETRHEQ across a wide range of h values, meaning it must be capturing the first-order behavior reasonably well, despite treating h as a fixed parameter. Third, h does not appear in the nondimensionalized RH budget (equation (14)), so it does not affect our fundamental explanation of SFE, only the time to equilibrium.

One way in which neglected diurnal variability might impact our results is in the derivation of equation (5). Unlike the box model, which directly models the diel-average state of the ABL, ETRHEQ is based on subdaily observations of RH. For maximum simplicity, we neglect this variability in our derivation of equation (5). However, diurnal variation in RH is considerable over land Dai (2006). Differences between estimates of EF using equation (5) and the ETRHEQ algorithm (described in Salvucci & Gentine, 2013; Rigden & Salvucci, 2015) are likely explained by ignoring diurnal variability in the derivation. Therefore, while equation (5) is exactly equivalent to ETRHEQ under steady-state conditions, it can differ from ETRHEQ under time-varying conditions observed in the real world, complicating the link between SFE and ETRHEQ. The accuracy of equation (5) in real-world conditions will be investigated in a future study.

7. Conclusions

A major limitation to modeling ET is in parameterizing biophysical processes at the land surface that may limit ET, such as water limitation. Recent work, including work on the ETRHEQ method, has shown empirically that quite accurate estimates of ET can be obtained at daily time scales solely using routine weather station observations, with no surface data required. While this is a major benefit over previous

methods—which either require land surface information as inputs or only apply to well-watered land surfaces—it has lacked a physical explanation. It is also somewhat unexpected, since land surface conditions often limit ET. One possible explanation is that the atmospheric state is sensitive to surface conditions, such that surface conditions become encoded in the atmospheric state, reminiscent of historical work on equilibrium ET. Much of the literature on equilibrium ET focuses on simple box models. In this study, we have parsimoniously built on this literature to present a box model—modified to include generic cooling and drying terms, which can represent, for example, radiative cooling and water vapor divergence, respectively—that reproduces ETRHEQ over a wide range of conditions. We show that ETRHEQ is exactly equivalent to assuming a balance between the surface moistening and heating terms in the box's relative humidity budget. There is good reason to believe that these terms will balance, at least approximately, under a broad range of conditions, due to the sensitivity of the atmospheric state to surface fluxes. In addition to providing a physical explanation for the success of ETRHEQ, this work has potential for diagnosing and correcting known biases in ET in climate models (Mueller & Seneviratne, 2014) that are likely caused, in part, by errors in parameterizations of water limitation at the land surface.

Appendix A: Derivation of Steady-State ETRHEQ Solution

In this section, we derive a simplified expression for the ETRHEQ hypothesis applied to the idealized box model presented in the main text at steady state.

A.1. Penman-Monteith Equation for g_s

Linearizing $q^*(T_S)$ around $T_S = \theta_M$ gives

$$q^*(T_S) \approx q^*(\theta_M) + \Delta(T_S - \theta_M) \tag{A1}$$

where $\Delta = \left.\frac{\partial q^*}{\partial T}\right|_{\theta_M}$. Combining equations (8)–(10) and (A1) gives the Penman-Monteith equation (Monteith, 1965; Penman, 1948)

$$\lambda E = \frac{\Delta(R_n - G) + \rho c_p g_a (q^*(\theta_M) - q_M)}{\Delta + \gamma(1 + \frac{g_a}{g_s})} \tag{A2}$$

which can be rearranged to give an expression for g_s

$$g_s = \frac{g_a \gamma \lambda E}{\Delta(R_n - G) - (\Delta + \gamma)\lambda E + \rho g_a c_p (q^*(\theta_M) - q_M)} \tag{A3}$$

or equivalently

$$g_s = \frac{g_a(R_n - G - H)}{g_a \lambda \rho (q^*(\theta_M) - q_M) - (R_n - G - (1 + \frac{\Delta}{\gamma})H)} \tag{A4}$$

where $\gamma = \frac{c_p}{\lambda}$.

A.2. ETRHEQ Solution for g_s

Rearranging equation (10) gives

$$q_S = \frac{g_a q_M + g_s q^*(T_S)}{g_a + g_s} \tag{A5}$$

Dividing through by $q^*(T_S)$ gives

$$RH_S = \frac{RH_M \frac{q^*(\theta_M)}{q^*(T_S)} + \frac{g_s}{g_a}}{1 + \frac{g_s}{g_a}} \tag{A6}$$

Applying equations (A1) and (A2) and (8) and (9) gives

$$RH_S = \frac{RH_M \frac{q^*(\theta_M)}{R_n - G - \frac{\Delta(R_n - G) + \rho c_p g_a (q^*(\theta_M) - q_M)}{\Delta + \gamma(1 + \frac{g_a}{g_s})}} + \frac{g_s}{g_a}}{1 + \frac{g_s}{g_a}} \quad \text{(A7)}$$

Substituting equation (A7) into the steady-state ETRHEQ condition (equation (4)) and simplifying gives

$$\bar{g}_s^{\text{ETRHEQ}} = \frac{g_a}{1 + \frac{\lambda \rho g_a q^*(\theta_M)}{\epsilon(R_n - G)}(1 + \epsilon RH_M)} \frac{RH_M}{1 - RH_M} \quad \text{(A8)}$$

A.3. ETRHEQ Solution for EF

Setting the two equations for g_s (equations (A4) and (A8)) equal to one another and solving for H gives

$$H = \frac{c_p q^*(\theta_M)(R_n - G)}{\Delta \lambda q_M + c_p q^*(\theta_M)} \quad \text{(A9)}$$

This simplifies to the final expression

$$EF = \frac{RH\epsilon}{RH\epsilon + 1} \quad \text{(A10)}$$

Appendix B: Derivation of RH Budget

In this section, we derive the nondimensionalized relative humidity budget given in equation (14). The relative humidity at screen level (typically taken as 2 m above the surface) is defined as $RH = q_M/q^*(T)$, where T is air temperature at screen level. To a good approximation, $T = \theta_M$ at screen level, so we may write $RH = q_M/q^*(\theta_M)$ at screen level. Note that this relation does not hold far from the surface in the box model, where $T(z) < \theta_M$.

Using the definition of RH, the chain rule and prognostic equations for θ_M and q_M given in equations (6) and (7), respectively, yields the expression

$$\frac{\mathrm{d}RH}{\mathrm{d}t} = \frac{\partial RH}{\partial \theta_M}\frac{d\theta_M}{\mathrm{d}t} + \frac{\partial RH}{\partial q_M}\frac{\mathrm{d}q_M}{\mathrm{d}t} = \frac{1}{hq^*(\theta_M)}\left(\frac{\lambda E - RH\epsilon H}{\rho\lambda} + g_r(q_R - q_M) - \frac{c_p}{\lambda}RH\epsilon g_r(\theta_R - \theta_M)\right) \quad \text{(B1)}$$

We now nondimensionalize this equation. The relevant dimensionless variables are

$$\hat{q} = \frac{q\rho\lambda g_a}{R_n - G}$$
$$\hat{t} = \frac{tg_a}{h}$$
$$\hat{T} = \frac{T\rho c_p g_a}{R_n - G}$$
$$\hat{\Delta} \equiv \frac{\partial \hat{q}^*}{\partial \hat{T}} = \Delta\frac{\lambda}{c_p} \equiv \epsilon$$
$$\hat{RH} \equiv \frac{\hat{q}}{\hat{q}^*(T)} = RH$$
$$\hat{H} \equiv \hat{T}_s - \hat{\theta}_M = \frac{\rho c_p g_a (T_s - \theta_M)}{R_n - G}$$
$$\lambda\hat{\mathrm{E}} \equiv \frac{1}{g_a}\frac{g_s g_a}{g_s + g_a}(\hat{q}^*(T_s) - \hat{q}_M) = \frac{\lambda\rho\frac{g_s g_a}{g_s + g_a}(q^*(T_s) - q_M)}{R_n - G}$$

We have treated $R_n - G$ as a fixed constant, as is conventional, although it varies with surface temperature. Substituting these expressions into equation (B1) yields the nondimensionalized RH equation

$$\hat{q}^*(\theta_M)\frac{\mathrm{d}\hat{RH}}{\mathrm{d}\hat{t}} = \lambda\hat{\mathrm{E}} - \hat{RH}\hat{\Delta}\hat{H} + \frac{g_r}{g_a}\left((\hat{q}_R - \hat{q}_M) - \hat{RH}\hat{\Delta}(\hat{\theta}_R - \hat{\theta}_M)\right)$$

Acknowledgments
K. A. M. acknowledges funding from a Winokur Seed Grant in Environmental Sciences from the Harvard University Center for the Environment. We thank Zhiming Kuang for helpful feedback on a draft manuscript. No data were used in this study.

References

Aubinet, M., Vesala, T., & Papale, D. (Eds.) (2012). *Eddy covariance Edited by* Aubinet, M., Vesala, T., & Papale, D.Dordrecht: Springer Netherlands. https://doi.org/10.1007/978-94-007-2351-1

Bateni, S. M., & Entekhabi, D. (2012). Relative efficiency of land surface energy balance components. *Water Resources Research*, *48*, W04510. https://doi.org/10.1029/2011WR011357/abstract

Betts, A. K. (1994). Relation between equilbrium evaporation and the saturation pressure budget. *Boundary-Layer Meteorology*, *71*, 235–245.

Betts, A. K. (2000). Idealized model for equilibrium boundary layer over land. *Journal of Hydrometeorology*, *1*(6), 507–523. https://doi.org/10.1175/1525-7541(2000)001<0507:IMFEBL>2.0.CO;2

Betts, A. K., & Chiu, J. C. (2010). Idealized model for changes in equilibrium temperature, mixed layer depth, and boundary layer cloud over land in a doubled CO_2 climate. *Journal of Geophysical Research*, *115*, D19108. https://doi.org/10.1029/2009JD012888

Blossey, P. N., Bretherton, C. S., Zhang, M., Cheng, A., Endo, S., Heus, T., et al. (2013). Marine low cloud sensitivity to an idealized climate change: The CGILS LES intercomparison. *Journal of Advances in Modeling Earth Systems*, *5*, 234–258. https://doi.org/10.1002/jame.20025

Byrne, M. P., & O'Gorman, P. A. (2016). Understanding decreases in land relative humidity with global warming: Conceptual model and GCM simulations. *Journal of Climate*, *29*(24), 9045–9061. https://doi.org/10.1175/JCLI-D-16-0351.1

Cronin, T. W. (2013). A sensitivity theory for the equilibrium boundary layer over land: Boundary layer sensitivity theory. *Journal of Advances in Modeling Earth Systems*, *5*, 764–784. https://doi.org/10.1002/jame.20048

Culf, A. D. (1994). Equilibrium evaporation beneath a growing convective boundary layer. *Boundary-Layer Meteorology*, *70*(1-2), 37–49. https://doi.org/10.1007/BF00712522

D'Andrea, F., Provenzale, A., Vautard, R., & Noblet-Decoudre, N. D. (2006). Hot and cool summers: Multiple equilibria of the continental water cycle. *Geophysical Research Letters*, *33*, L24807. https://doi.org/10.1029/2006GL027972

Dai, A. (2006). Recent climatology, variability, and trends in global surface humidity. *Journal of Climate*, *19*(15), 3589–3606. https://doi.org/10.1175/JCLI3816.1

De Bruin, H. a. R. (1983). A model for the Priestley-Taylor parameter Î±. *Journal of Climate and Applied Meteorology*, *22*(4), 572–578. https://doi.org/10.1175/1520-0450(1983)022<0572:AMFTPT>2.0.CO;2

Deremble, B., Wienders, N., & Dewar, W. K. (2012). CheapAML: A simple, atmospheric boundary layer model for use in ocean-only model calculations. *Monthly Weather Review*, *141*(2), 809–821. https://doi.org/10.1175/MWR-D-11-00254.1

Driedonks, A. G. M. (1982). Sensitivity analysis of the equations for a convective mixed layer. *Boundary-Layer Meteorology*, *22*(4), 475–480. https://doi.org/10.1007/BF00124706

Emanuel, K. A. (1995). The behavior of a simple hurricane model using a convective scheme based on subcloud-layer entropy equilibrium. *Journal of the Atmospheric Sciences*, *52*(22), 3960–3968. https://doi.org/10.1175/1520-0469(1995)052<3960:TBOASH>2.0.CO;2

Emanuel, K. A., & Zivkovic-Rothman, M. (1999). Development and evaluation of a convection scheme for use in climate models. *Journal of the Atmospheric Sciences*, *56*(11), 1766–1782. https://doi.org/10.1175/1520-0469(1999)056<1766:DAEOAC>2.0.CO;2

Gentine, P., Chhang, A., Rigden, A., & Salvucci, G. (2016). Evaporation estimates using weather station data and boundary layer theory. *Geophysical Research Letters*, *43*, 11,661–11,670. https://doi.org/10.1002/2016GL070819

Gentine, P., Ferguson, C. R., & Holtslag, A. A. M. (2013). Diagnosing evaporative fraction over land from boundary-layer clouds. *Journal of Geophysical Research: Atmospheres*, *118*, 8185–8196. https://doi.org/10.1002/jgrd.50416/abstract

Green, J. K., Seneviratne, S. I., Berg, A. M., Findell, K. L., Hagemann, S., Lawrence, D. M., & Gentine, P. (2019). Large influence of soil moisture on long-term terrestrial carbon uptake. *Nature*, *565*(7740), 476–479. https://doi.org/10.1038/s41586-018-0848-x

Humphrey, V., Zscheischler, J., Ciais, P., Gudmundsson, L., Sitch, S., & Seneviratne, S. I. (2018). Sensitivity of atmospheric CO_2 growth rate to observed changes in terrestrial water storage. *Nature*, *560*(7720), 628–631. https://doi.org/10.1038/s41586-018-0424-4

Jarvis, P. G., & McNaughton, K. G. (1986). Stomatal control of transpiration: Scaling up from leaf to region. *Advances in Ecological Research*, *15*, 1–49. https://doi.org/10.1016/S0065-2504(08)60119-1

Ma, H.-Y., Klein, S., Xie, S., Zhang, C., Tang, S., Tang, Q., et al. (2018). CAUSES: On the role of surface energy budget errors to the warm surface air temperature error over the Central United States. *Journal of Geophysical Research: Atmospheres*, *123*, 2888–2909. https://doi.org/10.1002/2017JD027194

McNaughton, K. G. (1976b). Evaporation and advection II: Evaporation downwind of a boundary separating regions having different surface resistances and available energies. *Quarterly Journal of the Royal Meteorological Society*, *102*(431), 193–202. https://doi.org/10.1002/qj.49710243116

McNaughton, K. G. (1976a). Evaporation and advection I: Evaporation from extensive homogeneous surfaces. *Quarterly Journal of the Royal Meteorological Society*, *102*(431), 181–191. https://doi.org/10.1002/qj.49710243115

McNaughton, K. G., & Spriggs, T. W. (1986). A mixed-layer model for regional evaporation. *Boundary-Layer Meteorology*, *34*(3), 243–262. https://doi.org/10.1007/BF00122381

Monteith, J. L. (1965). Evaporation and environment. *Symposia of the Society for Experimental Biology*, *19*, 205–234 eng.

Monteith, J. L. (1981). Evaporation and surface temperature. *Quarterly Journal of the Royal Meteorological Society*, *107*(451), 1–27. https://doi.org/10.1002/qj.49710745102

Mueller, B., & Seneviratne, S. I. (2014). Systematic land climate and evapotranspiration biases in CMIP5 simulations. *Geophysical Research Letters*, *41*, 128–134. https://doi.org/10.1002/2013GL058055/abstract

Novick, K. A., Ficklin, D. L., Stoy, P. C., Williams, C. A., Bohrer, G., Oishi, A. C., et al. (2016). The increasing importance of atmospheric demand for ecosystem water and carbon fluxes. *Nature Climate Change*, *6*(11), 1023–1027. https://doi.org/10.1038/nclimate3114

Pauluis, O., & Held, I. M. (2002). Entropy budget of an atmosphere in radiative-convective equilibrium. Part I: Maximum work and frictional dissipation. *Journal of the Atmospheric Sciences*, *59*(2), 125–139. https://doi.org/10.1175/1520-0469(2002)059<0125:EBOAAI>2.0.CO;2

Penman, H. L. (1948). Natural evaporation from open water, bare soil and grass. *Proceedings of the Royal Society of London. Series A. Mathematical and Physical Sciences*, *193*(1032), 120–145. https://doi.org/10.1098/rspa.1948.0037

Priestley, C. H. B., & Taylor, R. J. (1972). On the assessment of surface heat flux and evaporation using large-scale parameters. *Monthly Weather Review*, *100*(2), 81–92. https://doi.org/10.1175/1520-0493(1972)100<0081:OTAOSH>2.3.CO;2

Raupach, M. R. (2000). Equilibrium evaporation and the convective boundary layer. *Boundary-Layer Meteorology*, *96*(1-2), 107–142. https://doi.org/10.1023/A:1002675729075

Raupach, M. R. (2001). Combination theory and equilibrium evaporation. *Quarterly Journal of the Royal Meteorological Society*, *127*(574), 1149–1181.

Raymond, D. J. (1995). Regulation of moist convection over the West Pacific warm pool. *Journal of the Atmospheric Sciences*, *52*(22), 3945–3959. https://doi.org/10.1175/1520-0469(1995)052<3945:ROMCOT>2.0.CO;2

Rieck, M., Nuijens, L., & Stevens, B. (2012). Marine boundary layer cloud feedbacks in a constant relative humidity atmosphere. *Journal of the Atmospheric Sciences*, *69*(8), 2538–2550. https://doi.org/10.1175/JAS-D-11-0203.1

Rigden, A. J., & Salvucci, G. D. (2015). Evapotranspiration based on equilibrated relative humidity (ETRHEQ): Evaluation over the continental U.S. *Water Resources Research*, *51*, 2951–2973. https://doi.org/10.1002/2014WR016072/abstract

Rigden, A. J., & Salvucci, G. D. (2017). Stomatal response to humidity and CO_2 implicated in recent decline in US evaporation. *Global Change Biology*, *23*(3), 1140–1151. https://doi.org/10.1111/gcb.13439/abstract

Salvucci, G. D., & Gentine, P. (2013). Emergent relation between surface vapor conductance and relative humidity profiles yields evaporation rates from weather data. *Proceedings of the National Academy of Sciences*, *110*(16), 6287–6291. https://doi.org/10.1073/pnas.1215844110

Seager, R., Blumenthal, M. B., & Kushnir, Y. (1995). An advective atmospheric mixed layer model for ocean modeling purposes: Global simulation of surface heat fluxes. *Journal of Climate*, *8*(8), 1951–1964. https://doi.org/10.1175/1520-0442(1995)008<1951:AAAMLM>2.0.CO;2

Shuttleworth, W. J., & Calder, I. R. (1979). Has the Priestley-Taylor equation any relevance to forest evaporation? *Journal of Applied Meteorology*, *18*(5), 639–646. https://doi.org/10.1175/1520-0450(1979)018<0639:HTPTEA>2.0.CO;2

Slatyer, R. O., & McIlroy, I. C. (1961). *Practical microclimatology: With special reference to the water factor in soil-plant-atmosphere relationships*. Melbourne, Australia: Commonwealth Scientific and Industrial Research Organisation.

Vallis, G. K., Parker, D. J., & Tobias, S. M. (2019). A simple system for moist convection: The Rainy-Benard model. *Journal of Fluid Mechanics*, *862*, 162–199. https://doi.org/10.1017/jfm.2018.954

van Heerwaarden, C. C., VilÃ-Guerau de Arellano, J., Moene, A. F., & Holtslag, A. M. (2009). Interactions between dry-air entrainment, surface evaporation and convective boundary-layer development. *Quarterly Journal of the Royal Meteorological Society*, *135*(642), 1277–1291. https://doi.org/10.1002/qj.431

van Stratum, B. J. H., Vila-Guerau de Arellano, J., van Heerwaarden, C. C., & Ouwersloot, H. G. (2014). Subcloud-layer feedbacks driven by the mass flux of shallow cumulus convection over land. *Journal of the Atmospheric Sciences*, *71*(3), 881–895. https://doi.org/10.1175/JAS-D-13-0192.1

Zhou, S., Zhang, Y., Williams, A. P., & Gentine, P. (2019). Projected increases in intensity, frequency, and terrestrial carbon costs of compound drought and aridity events. *Science Advances*, *5*(1), eaau5740. https://doi.org/10.1126/sciadv.aau5740